Available online at www.sciencedirect.com

SCIENCE DIRECT®

International Journal of Mass Spectrometry 241 (2005) 25–29

International Journal of Mass Spectrometry

www.elsevier.com/locate/ijms

Femtosecond laser-induced dissociative ionization and Coulomb explosion of ethanol

Jianxin Chen, Ri Ma, Haizhen Ren, Xia Li, Hong Yang, Qihuang Gong*

State Key Laboratory for Mesoscopic Physics, Department of Physics, Peking University, Beijing 100871, PR China

Received 4 September 2004; accepted 20 October 2004
Available online 26 November 2004

Abstract

Using time-of-flight mass spectrometer, the femtosecond laser-induced dissociative ionization and Coulomb explosion of ethanol under irradiation of 130 fs pulse duration laser of linear and circular polarization at 810 nm, have been investigated. Coulomb explosion of C_2H_5OH molecule was observed to undergo a two-step process with one bond of the C—C—O skeleton atoms breaks firstly then the other. The similar laser intensity dependence of $C_2H_nOH^+$ ($n = 1$–4) ion yields and the molecular ion $C_2H_5OH^+$ indicated that they are the results of multiphoton ionization of inner-valence electrons followed by radiationless transitions to various dissociation channels of $C_2H_5OH^+$. By analyzing the momentum-scaled spectra, the intermediate daughter ions CH_2OH^+ and CH_3^+, $C_2H_5^+$ and OH^+ were concluded to be originated from the same Coulomb explosion channel of $C_2H_5OH^{2+}$ ion, respectively. The atomic ion C^{2+} showed an anisotropic angular distribution, which is reassessed to the geometric alignment mechanism.

Keywords: Coulomb explosion; Time-of-flight mass spectrum; Ethanol; Femtosecond laser

1. Introduction

Since tabletop femtosecond laser systems became commercially available, a large amount of research work has been done to investigate the interactions of molecules and intense laser fields. When a molecule was irradiated by laser light with an intensity of exceeding 10^{13} W/cm^2, one electron or several valence electrons may be stripped away through multiphoton ionization, tunnel ionization and over-the-barrier ionization (field ionization). Then dissociation or Coulomb explosion occur to form the ionic fragments. Many dynamical processes, such as the explosion pathway, the enhanced ionization and the spatial alignment, the structural deformation and explosion process, are understood for diatomic [1–4] and triatomic molecules [5–8] and polyatomic molecules with the special structures [9–13]. For polyatomic molecules, the signal intensity of the ionic fragments depended sensitively on the characteristics of incident laser fields [14–16]. Recently, Yamanouchi et al. have investigated the dissociative ionization of ethanol in the intense laser fields when the linear chirp rate of laser pulse changed. The light-dressed potential-energy surface at the singly charged stage has been elucidated to govern the nuclear dynamics [17]. Mathur et al. presented that the yields of singly and multiply charged atomic fragments from a series of alcohol molecules, from methanol and ethanol, through hexanol to dodecanol are suppressed when the circularly polarized light was used. Their experimental observation also indicated that the enhanced ionization mechanism holds for circularly polarized laser [18].

In this report, the femtosecond laser-induced dissociative ionization and Coulomb explosion of ethanol molecule were experimentally studied by means of time-of-flight (TOF) mass spectrometer. The characteristics of the ionic fragments coming from the field ionization and Coulomb explosion are analyzed. The dependences of the ionic fragments on the polarization of laser are also observed and discussed.

---

* Corresponding author. Tel.: +86 1062765884; fax: +86 1062756567.
E-mail address: qhgong@pku.edu.cn (Q. Gong).

1387-3806/$ – see front matter © 2004 Elsevier B.V. All rights reserved.
doi:10.1016/j.ijms.2004.10.021

2. Experimental setup

The experimental setup has been described in detail in our previous reports [19,20]. The employed laser system was a CPA femtosecond Ti:sapphire laser with a central wavelength of 810 nm, pulse duration of 130 fs and a repetition rate of 10 Hz. The maximum pulse energy can reach 5 mJ. A home-made TOF mass spectrometer with a 35 cm long field-free drift tube was used for ion analysis. The femtosecond laser pulses were focused into the vacuum chamber of the TOF mass spectrometer by a lens with a focal length of 150 mm. A gaseous sample was introduced into the vacuum chamber via a pulsed valve with a 0.2 mm orifice. The produced ions were accelerated by a two-stage electric field and detected by a micro-channel plate (MCP). The high transmission grids are installed in the mass spectrometer to collect the ion. The collecting radius of MCP is about 18 mm. The optimum mass resolution can reach 116 at $m/z = 58$. The signals were recorded using a 1 GHz data acquisition card and then transferred to a PC for storage and analysis. A half-wave plate was inserted into the path of the laser beam in order to rotate the laser polarization direction with respect to the detection axis of the TOF mass spectrometer. A quarter-wave plate was inserted into the path of the laser beam in order to obtain the desired laser ellipticity. The pulsed valve, the data acquisition card and the femtosecond laser pulses were timing scheduled by a DG535 digital delay and pulse generator.

3. Results and discussion

3.1. TOF mass spectra under different laser polarization

The typical TOF mass spectrum of ethanol induced by 810 nm, 130 fs linearly polarized laser pulses at a laser intensity of 3.8×10^{15} W/cm^2 is shown in Fig. 1. The laser polarization direction was collinear with the TOF mass spectrometer axis. The ionic fragments may be divided into three kinds. The first kind of ions refers to $C_2H_nOH^+$ ($n = 1$–5), which have the C–C–O skeleton. The second kind of ions is CH_2OH^+ and $C_2H_n^+$($n = 2, 3, 5$), which have either the C–C bond or C–O bond when one bond of the C–C–O skeleton breaks. The last kind of ionic fragments is CH_n^+($n = 1$–3), CH_2^{2+}, H_n^+($n = 1$–2), O^{n+} ($n = 1$–2), OH^+ and C^{n+} ($n = 1$–3). They have neither the C–C bond nor C–O bond.

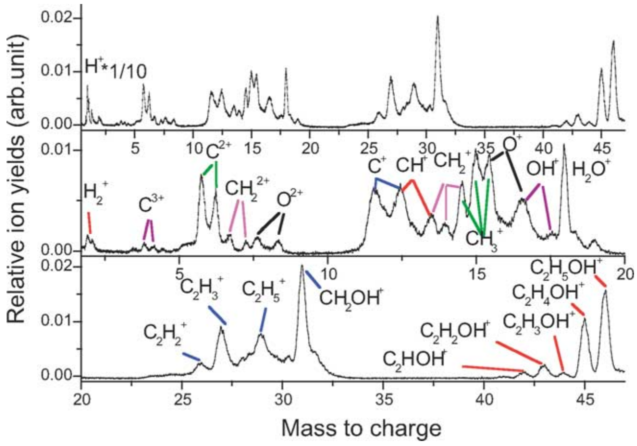

Fig. 1. A typical TOF mass spectrum of ethanol induced by 810 nm, 130 fs linearly polarized laser pulses at an intensity of 3.8×10^{15} W/cm^2. The laser polarization direction was collinear with the TOF mass spectrometer axis.

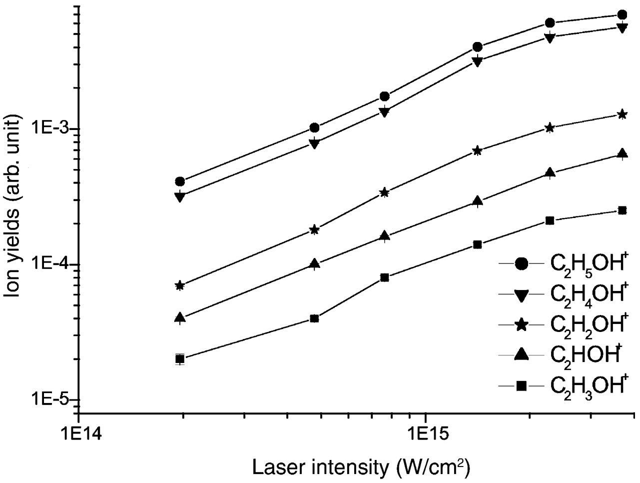

Fig. 2. The signal yields of $C_2H_nOH^+$($n = 1$–5) ions as a function of laser intensity.

Fig. 2 presents the signal intensities of $C_2H_nOH^+$($n =$ 1 5)ions, of which the C–C–O skeleton atoms are not destroyed, as a function of laser intensity. They exhibited the same dependences of ion yields on laser intensity, which are consistent with the results of C_2H_4 [21] and CH_3OH [22] molecules. This concluded that the observed $C_2H_nOH^+$ ($n = 1$–4) ions occurred as a result of multiphoton ionization of inner-valence electrons followed by radiationless transitions to various dissociation channels of the molecular ion $C_2H_5OH^+$. The intermediate daughter ions CH_2OH^+, $C_2H_5^+$,CH_3^+, and OH^+ have a double-peak or a triple-peak structure in the mass spectrum. These indicated that Coulomb explosion of C_2H_5OH molecule undergoes a two-step process. One bond of the C–C–O skeleton atoms breaks firstly then the other does. This is similar to that of C_3H_8 molecule in intense femtosecond laser fields [23].

Both vertically linear polarization and circular polarization laser were also used to investigate the Coulomb explosion of C_2H_5OH molecule. Fig. 3 shows the obtained TOF mass spectra when the laser polarization vector is parallel (in the upper trace) and perpendicular (in the middle trace) to the TOF mass spectrometer axis and when the laser pulse is circular (in the lower trace) at the same intensity. The signal intensity of H^+ ion was multiplied by a factor of $\frac{1}{10}$. There is no difference for the ion intensity of $C_2H_nOH^+$ ($n = 1$–5) in the horizontally and vertically linear polarization. While atomic ion C^{n+} ($n = 1$–3) yields decrease apparently in vertical polarization comparing with that in horizontal polarization, which reveals the result of molecular spatial alignment

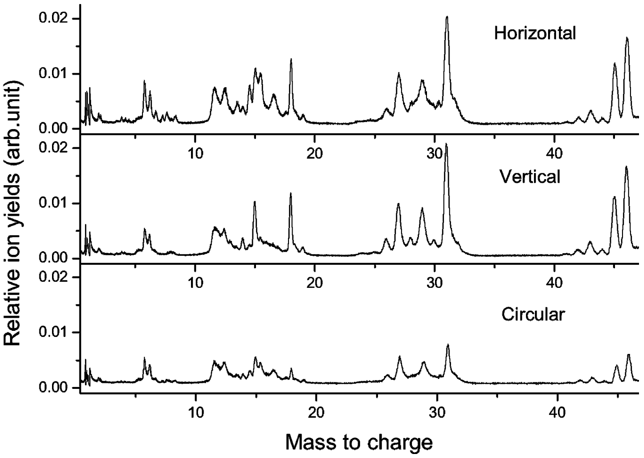

Fig. 3. The obtained TOF mass spectra when the laser polarization vector is parallel (in the upper trace) and perpendicular (in the middle trace) to the TOF mass spectrometer axis and when the laser pulse is circular (in the lower trace) at the same intensity. The signal intensity of H^+ ion was multiplied by a factor of $\frac{1}{10}$.

in intense laser fields. A significant decrease of ionization for the circularly polarized laser is also observed in comparing with the linearly polarized laser. It is consistent with the conclusion of Ref. [18]. The kinds of ionic fragments under three different laser polarizations are identical. This indicates that the polarization property of laser beam do not affect the two-step Coulomb explosion process of C_2H_5OH molecule in intense laser fields.

3.2. The momentum-scaled spectra of intermediate daughter ions

The signals of CH_2OH^+ and CH_3^+ ions exhibit three peaks, the forward, middle and backward ion peaks. The forward and backward peaks are formed by ions initially moving toward and backward the detector. They can be used to calculate the kinetic energy release (KER) [24]. The equation is given by

$$E_{\mathrm{KER}} = \frac{(U_1 - U_2)^2}{8md^2} q^2 \Delta t^2,$$

where U_1 is the potential voltage of the repeller plate, U_2 is that for the first acceleration plate, d is the distance between these plates, q is the charge of the ion, and Δt is the difference in the arrival times between the forward and backward accelerated ions. If we assume that t_0 is the flight time at the center of these two peaks corresponding to zero momentum. The measured TOF mass spectrum can be transformed into the momentum-scaled spectrum along the direction parallel to the TOF mass spectrometer axis by using the following equation,

$$P_{//} = \frac{q(U_1 - U_2)(t - t_0)}{d},$$

The momentum-scaled mass spectrum can help us identify the Coulomb explosion pathway of doubly charged ethanol ion $C_2H_5OH^{2+}$. Fig. 4 shows the momentum-scaled spectra of intermediate daughter ions CH_2OH^+ and CH_3^+. It is clearly noted that the forward and backward ion peaks of CH_2OH^+ and CH_3^+ ions have the same released momentum, $|P_{//}| = 88,000\,\mathrm{amu\,m/s}$. It indicated that they originated from the same Coulomb explosion channel of $C_2H_5OH^{2+}$ ion, $C_2H_5OH^{2+} \rightarrow CH_3^+ + CH_2OH^+$. We also gave the momentum-scaled spectra of intermediate daughter ions $C_2H_5^+$ and OH^+ ions in the same way (as shown in Fig. 5). The peaks for forward and backward $C_2H_5^+$ and backward OH^+ are multiplied by a factor of 1.3, 1.3, 1.1, respectively. The momentum of the forward ion for $C_2H_5^+$ and OH^+ ions is 83,000 amu m/s. This also suggested that they arose from the same Coulomb explosion channel of $C_2H_5OH^{2+}$ ion, that is $C_2H_5OH^{2+} \rightarrow C_2H_5^+ + OH^+$. The middle ion peaks of CH_2OH^+, $C_2H_5^+$, and CH_3^+ are the results of "soft" dissociation of singly charged ion $C_2H_5OH^+$ such as the following dissociative channels: $CH_3CH_2OH^+ \rightarrow CH_2OH^+ + CH_3$, $CH_3CH_2OH^+ \rightarrow CH_3^+ + CH_2OH$, $CH_3CH_2OH^+ \rightarrow C_2H_5^+ + OH$, etc.

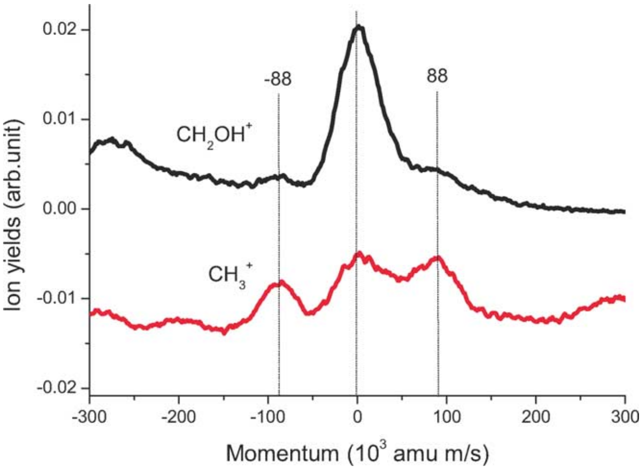

Fig. 4. The momentum-scaled spectra of intermediate daughter ions CH_2OH^+ andCH_3^+.

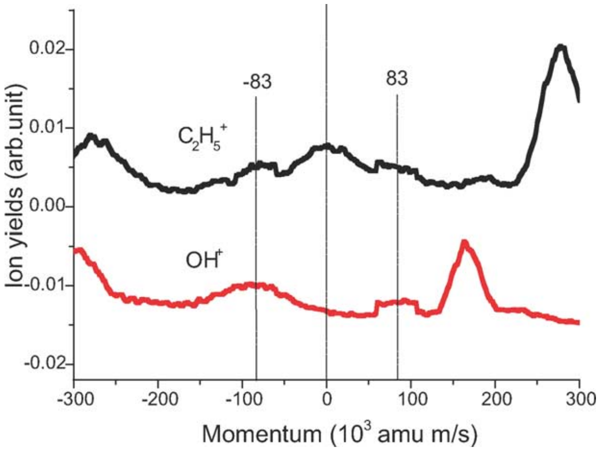

Fig. 5. The momentum-scaled spectra of intermediate daughter ions $C_2H_5^+$ and OH^+. The peaks for forward and backward $C_2H_5^+$ and backward OH^+ are multiplied by a factor of 1.3, 1.3, 1.1, respectively.

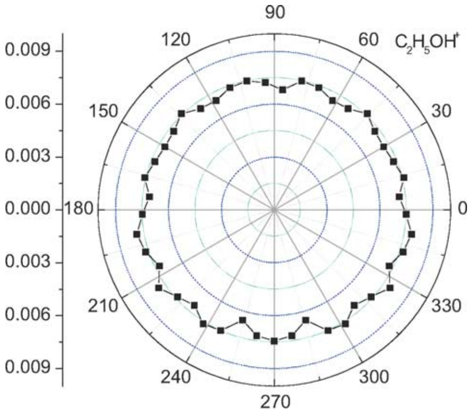

Fig. 6. The angular distribution of the molecular ion $C_2H_5OH^+$ at a laser intensity of 3.8×10^{15} W/cm^2.

3.3. *Angular distributions of the molecular ion $C_2H_5OH^+$ and atomic ion C^{2+}*

The angular distributions of the $C_2H_5OH^+$ and C^{2+} ions at a laser intensity of 3.8×10^{15} W/cm^2 are shown in Figs. 6 and 7, respectively. The angular distribution of the molecular ion $C_2H_5OH^+$ exhibits spatial isotropy. While the signal intensity of the atomic ion C^{2+} is maximum in the direction of the laser polarization vector and minimum in the orthogonal direction. The dynamic and geometric alignment mechanisms have been proposed to explain the anisotropic angular distribution of the atomic ion [25,26]. It is significant importance to reassess the contribution of these two mechanisms to the observed anisotropic angular distribution of the ionic fragments. The method that introduced by Ellent et al. was used to evaluate which alignment mechanism is predominant in our experiment [27]. Fig. 8 presents the TOF mass spectra in horizontally linear polarization and circular polarization with equal electric field along the detection axis of the TOF mass spectrometer. The signal intensity of H^+ ion was multiplied by a factor of $\frac{1}{10}$. The signal intensity of C^{2+} ion coming from the Coulomb explosion of ethanol molecule in circular polarization is about 1.1 ± 0.1 times higher than that in horizontally linear polarization. The nearly identical signal intensity suggested that the geometric alignment is dominant under our experimental conditions.

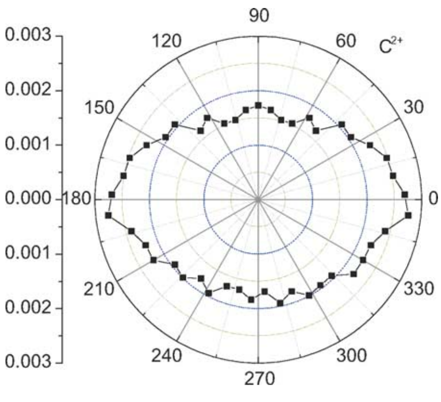

Fig. 7. The angular distribution of the atomic ion C^{2+} at a laser intensity of 3.8×10^{15} W/cm^2.

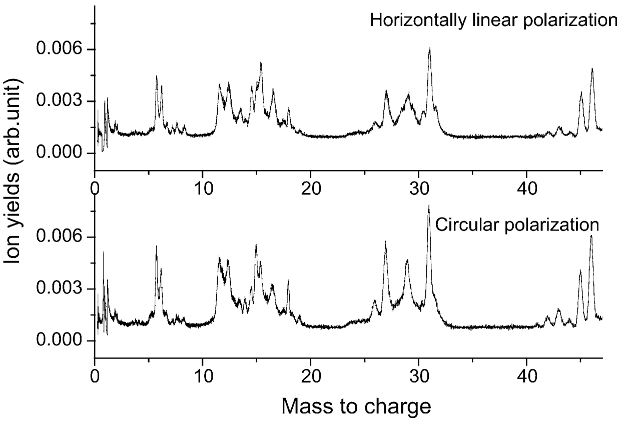

Fig. 8. The TOF mass spectra in horizontally linear polarization and circular polarization with equal electric field along the detection axis of the TOF mass spectrometer. The signal intensity of H^+ ion was multiplied by a factor of $\frac{1}{10}$.

The ratio of C^{2+} ion yield in the direction of the laser polarization vector and the orthogonal direction is 1.6. The other two reasons are also responsible for it except for the molecular geometric alignment: Coulomb explosion of the ethanol molecule undergoes a two-step process and the angle between the C–C bond and the C–O bond is 109.4° in the structure of the ethanol molecule. These effects lead to the reduction of the ratio of C^{2+} ion yield with a parallel polarization versus orthogonal polarization.

4. Summary

Femtosecond laser-induced dissociative ionization and Coulomb explosion of C_2H_5OH have been studied by using TOF mass spectrometer. The ionic fragments in the whole mass spectrum present apparent characteristics. The $C_2H_nOH^+$ ($n = 1$–4) ions were assigned to the various dissociation channels of the molecular ion $C_2H_5OH^+$. The appearances of intermediate daughter ions CH_2OH^+, $C_2H_5^+$, CH_3^+, and OH^+ with a double peak or a triple peak structure indicated that Coulomb explosion of C_2H_5OH molecule undergoes a two-step process. The momentum-scaled spectra were used to identify that CH_2OH^+ and CH_3^+, $C_2H_5^+$ and OH^+ ions originated from the same Coulomb explosion channel of $C_2H_5OH^{2+}$ ion, respectively. The angular distribution of $C_2H_5OH^+$ ion presents spatial isotropy. While the C^{2+} ion shows the anisotropic angular distribution. By comparing the signal intensity of the C^{2+} ion in horizontally linear polarization and circular polarization with equal electric field along the detection axis of the TOF mass spectrometer, we concluded that the geometric alignment mechanism is dominant under our experimental conditions.

Acknowledgements

This work supported by the National Key Basic Research Special Foundation (NKBRSF) under grant no. TG1999075207, the National Natural Science Foundation of China under grant nos. 10104003, 90206003 and 90101027, and the China Postdoctoral Science Foundation (2003034093).

References

[1] K. Miyazaki, T. Shimizu, D. Normand, J. Phys. B: At. Mol. Opt. Phys. 37 (2004) 753.
[2] M. Schmidt, D. Normand, C. Cornaggia, Phys. Rev. A 50 (1994) 5037.
[3] Ph. Hering, C. Cornaggia, Phys. Rev. A 59 (1999) 2836.
[4] F. Rosca-Pruna, E. Springate, H.L. Offerhaus, M. Krishnamurthy, N. Farid, C. Nicode, M.J.J. Vrakking, J. Phys. B: At. Mol. Opt. Phys. 34 (2001) 4919.
[5] P. Graham, K.W.D. Ledingham, R.P. Singhal, T. McCanny, S.M. Hankin, X. Fang, D.J. Smith, C. Kosmidis, P. Tzallas, A.J. Langley, P.F. Taday, J. Phys. B: At. Mol. Opt. Phys. 32 (1999) 5557.
[6] S. Couris, E. Koudoumas, S. Leach, C. Fotakis, J. Phys. B: At. Mol. Opt. Phys. 32 (1999) L439.
[7] W.A. Bryan, J.H. Sanderson, A. El-Zein, W.R. Newell, P.F. Taday, A.J. Langley, J. Phys. B: At. Mol. Opt. Phys. 33 (2000) 745.
[8] S. Banerjee, G.R. Kumar, D. Mathur, Phys. Rev. A 60 (1999) R3369.
[9] J.H. Sanderson, R.V. Thomas, W.A. Bryan, W.R. Newell, P.F. Taday, A.J. Langley, J. Phys. B: At. Mol. Opt. Phys. 30 (1997) 4499.
[10] H.Z. Ren, R. Ma, X. Li, J.X. Chen, H. Yang, Q.H. Gong, Int. J. Mass Spectrom. 235 (2004) 117.
[11] S. Shimizu, J. Kou, S. Kawato, K. Shimizu, S. Sakabe, N. Nakashima, Chem. Phys. Lett. 317 (2000) 609.
[12] S. Shimizu, V. Zhakhovskii, F. Sato, S. Okihara, S. Sakabe, K. Nishihara, Y. Izawa, T. Yatsuhashi, N. Nakashima, J. Chem. Phys. 117 (2002) 3180.
[13] L. Poth, Q. Zhong, J.V. Ford, S.M. Hurley, A.W. Castleman Jr., Chem. Phys. 239 (1998) 309.
[14] X.-P. Tang, S.-F. Wang, M.E. Elshakre, L.-R. Gao, Y.-L. Wang, H.-F. Wang, F.-A. Kong, J. Phys. Chem. A 107 (2003) 13.
[15] R. Itakura, J. Watanabe, A. Hishikawa, K. Yamanouchi, J. Chem. Phys. 114 (2001) 5598.
[16] A.M. Muller, B. Witzel, C.J.G.J. Uiterwaal, J. Wanner, K.-L. Kompa, Phys. Rev. Lett. 88 (2002) 023001.
[17] R. Itakura, K. Yamanouchi, T. Tanabe, T. Okamoto, F. Kannari, J. Chem. Phys. 119 (2003) 4179.
[18] F.A. Rajgara, M. Krishnamurthy, D. Mathur, J. Chem. Phys. 119 (2003) 12224.
[19] C.Y. Wu, H.Z. Ren, T.T. Liu, R. Ma, H. Yang, H.B. Jiang, Q.H. Gong, Int. J. Mass. Spectrom. 216 (2002) 249.
[20] H.Z. Ren, C.Y. Wu, R. Ma, H. Yang, H.B. Jiang, Q.H. Gong, Int. J. Mass. Spectrom. 219 (2002) 305.
[21] A. Talebpour, A.D. Bandrauk, J. Yang, S.L. Chin, Chem. Phys. Lett. 313 (1999) 789.
[22] C.Y. Wu, H.Z. Ren, T.T. Liu, R. Ma, H. Yang, H.B. Jiang, Q.H. Gong, J. Phys. B: Atom. Mol. Opt. Phys. 35 (2002) 2575.
[23] J.X. Chen, R. Ma, X. Li, H.Z. Ren, H. Yang, Q.H. Gong, J. Phys. B: Atom. Mol. Opt. Phys. 37 (2004) 2501.
[24] J. Purnell, E.M. Snyder, S. Wei, A.W. Castleman Jr., Chem. Phys. Lett. 229 (1994) 333.
[25] J.H. Posthumus, J. Plumridge, M.K. Thomas, K. Codling, L.J. Frasinski, A.J. Langley, P.F. Taday, J. Phys. B: Atom. Mol. Opt. Phys. 31 (1998) 553.
[26] P. Dietrich, D.T. Strickland, M. Laberge, P.B. Corkum, Phys. Rev. A 47 (1993) 2305.
[27] Ch. Ellert, P.B. Corkum, Phys. Rev. A 59 (1999) 3170.